Table 1 Genital findings in Patients with MAMLD1 Deletions or Mutations

Patient	Patient 1	Patient 2	Patient 3	Patient 4	Patient 5	Patient 6	Patient 7	Patient 8	Patient 9	Patient 10	Patient 11	Patient 12
Deletion/Mutation	Deletion	Deletion	Deletion	Deletion	Deletion	Deletion	p.E124X	p.E124X	p.Q197X	p.R653X	p.E109fs121X	p.E109fs121X
Inheritance	Sporadic	Sporadic	Familial	Familial	Familial	Sporadic	Familial	Familial	Sporadic	Sporadic	Sporadic	Sporadic
Age at examination	Neonate	Neonate	Neonate	Neonate	Fetus	...	4 months	1 month	2 years	1 month	1 year	1 2/12 year
Ambiguity	Yes	No	No	No	No	No	No	No	No	No	No	No
Hypospadias	Yes	Yes	Yes	Yes	Yes	Yes	Yes	Yes	Yes	Yes	Yes	Yes
(Type)	Severe	Penoscrotal	Glandular	Penile	Penile	N.D.	Penoscrotal	Penoscrotal	Penoscrotal	Penoscrotal	Penile	Penoscrotal
Micropenis	Yes	N.D.	N.D.	N.D.	N.D.	N.D.	No	No	Yes	Yes	No	No
Cryptorchidism	Yes (B)	N.D.	Yes (R)	Yes (B)	N.D.	N.D.	Yes (B)	No	No	Yes (B)	Yes (B)	No
Scrotal abnormalities	Yes	N.D.	N.D.	N.D.	N.D.	N.D.	Yes	Yes	Yes	Yes	No	No
Other findings	Vaginal pouch											

Patients 1 & 2: cases 474 and 441 in Hu et al[2]; patient 3–5: cases III-1, III-2, and III-3 in Barsch et al[4]; patient 6: case CNM86 in Biancalana et al[5]; patients 7–10: cases 1–4 in Fukami et al[1]; and patients 11 and 12: cases 2 and 3 in Kalfa et al[11] N.D.: not described; B: bilateral; and R: right.

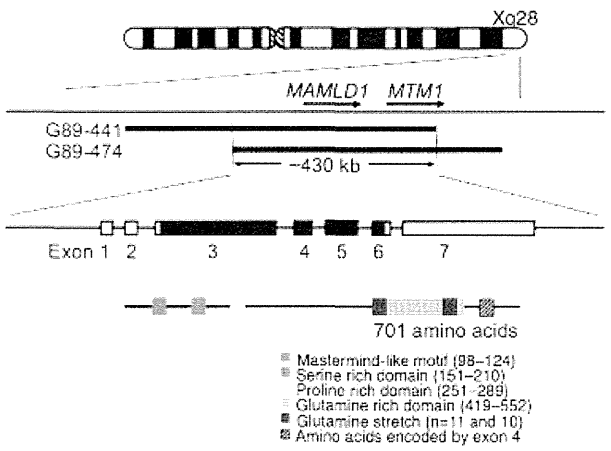

Figure 1 Positional cloning and the structure of *MAMLD1*. *MAMLD1* (*CXORF6*) has been isolated from a ~430 kb region commonly deleted in two patients with 46,XY DSD and myotubular myopathy (G89–441 and G89–474).[2] The horizontal bars indicate the deleted segments that involve *MAMLD1* and *MTM1* for myotubular myopathy. *MAMLD1* comprised 7 exons; the black and the white boxes represent the coding regions and the untranslated regions, respectively. MAMLD1 protein harbors mastermind-like domain and other characteristic domains.

within the smallest region of overlap in all patients with myotubular myopathy and 46,XY DSD,[7] and no other candidate gene for 46,XY DSD has been identified within the commonly deleted region. These findings imply that *MAMLD1* is an excellent candidate gene for 46,XY DSD.

MAMLD1 Mutations in 46,XY DSD Patients

The first evidence for *MAMLD1* being the causative gene for 46,XY DSD came from our group.[1] We performed direct sequencing for the coding exons 3–6 and their flanking splice sites of *MAMLD1* in 117 Japanese patients with various types of 46,XY DSD including 56 patients with hypospadias (16 with glandular type, 16 with penile type, 20 with pen scrotal type, and 4 with perineal type) associated with other external genital abnormalities, as well as in 49 European and Chinese patients with various types of abnormal genitalia ranging from hypospadias to feminized genitalia. Consequently, three nonsense mutations were identified in Japanese patients with hypospadias and other external abnormalities: p.E124X on exon 3 in two maternally related half brothers, p.Q197X on exon 3 in a sporadic patient, and p.R653X on exon 5 in a sporadic patient (patients 7–10 in ►**Table 1**).[1] The mothers of families A and C were heterozygous for the mutations, although the mother of family B was not studied.

The three nonsense mutations satisfy the conditions for the occurrence of nonsense mediated mRNA decay (NMD).[8] Consistent with this, RT-PCR from leukocytes indicated drastically reduced transcripts for the three nonsense mutations.[1] Furthermore, the NMD was prevented by the NMD inhibitor cycloheximide, providing further support for the occurrence of NMD in the three nonsense mutations. The occurrence of NMD was also demonstrated in the carrier mothers.[9] Thus, although the NMD has not been confirmed in the testicular

tissue, the results indicate that the three nonsense mutations are actually pathologic disease-causing mutations.

The occurrence of NMD would explain the apparently discordant genital phenotype between the patient with p.R653X and the Japanese patient with a microdeletion involving *MTM1* reported by Tsai et al.[10] In contrast to the p.R653X, the microdeletion resulted in the generation of a fusion gene between exons 1 to 4 of *MAMLD1* and exons 3 to 16 of *MTMR1* (locus order: *MAMLD1–MTM1–MTMR1*) that escaped NMD and was expressed at least in the muscle. Thus, although both the cases retained *MAMLD1* exons 1 to 4 and were missing *MAMLD1* exons 5 to 7, the patient with p.R653X had 46,XY DSD because of NMD, and the patient with the microdeletion had apparently normal genital development because of its positive expression.

Subsequently, Kalfa et al[11] have identified p.E109fs121X (c.325delG) that is predicted to undergo NMD in two of 41 41 patients with hypospadias of variable degrees (patients 11 and 12 in ←**Table 1**). Furthermore, several mutations confirmed by functional studies have been identified to date (our unpublished observation).

Additional substitutions have also been identified in patients with 46,XY DSD. First, Kalfa et al[11] identified p.V432A and p.531ins3Q (expansion of the second polyglutamine domain from 10 to 13) in single sporadic patients. However, both variants were detected in normal individuals by subsequent examination.[12] In addition, we performed functional studies for p.V432A using Hes3 (see below), and found apparently normal transcriptional activity (←**Fig. 2**). Second, Chen et al[12] identified p.Q529K, which could affect splicing, in a patient with severe hypospadias. However, no functional studies have been performed for p.Q529K. Third, Brandao et al[13] detected p.H432Q, which interestingly appears to have an increased rather than a decreased function, in 4 of 50 patients with 46,XY DSD. However, this substitution is registered as a polymorphism at present, indicating the presence of this substitution in apparently normal individuals. Thus, there is no direct evidence for these substitutions being pathologic mutations. Rather, these substitutions appear to be variations rather than mutations. Nevertheless, p.531ins3Q, which may affect the three-dimensional protein structure, could function as a susceptibility factor, as has been shown for the polyglutamine expansion in exon 1 of *AR* for androgen receptor.[14]

Taken together, it is obvious that *MAMLD1* is a causative gene for 46,XY DSD with hypospadias as a salient phenotype, because of the identification of nonsense mutations and a frameshift mutation that should be subject to NMD. Furthermore, it might be possible that the identified substitutions may function as susceptibility factors.

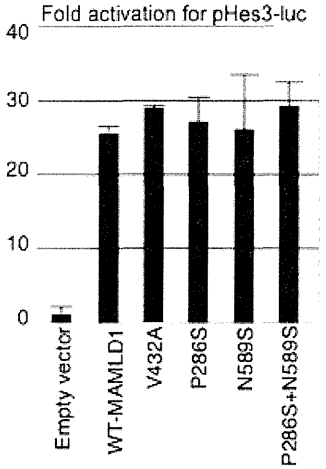

Figure 2 Functional studies for *MAMLD1* substitutions. The p.V432A, p.P286S, p.N589S, and p.P286S–p.N589S (S–S haplotype) have normal transactivating activities for the promoter of a non-canonical Notch target Hes3.

Phenotypes in Affected Patients

Genital findings in patients with microdeletions involving *MAMLD1* and in those with definitive intragenic *MAMLD1* mutations are shown in ←**Table 1**. Although detailed phenotypes are not examined in patients with microdeletions encompassing *MAMLD1*, affected patients almost invariably have hypospadias of variable degrees and often exhibit other genital features such as micropenis, cryptorchidism, and abnormal scrotum. Furthermore, patient 1 manifests rather ambiguous genitalia with virginal pouch, and patient 12 exhibits apparently isolated hypospadias phenotype. Thus, the phenotypic spectrum of *MAMLD1* mutations appears to be somewhat variable, with hypospadias as the core genital abnormality.

Detailed endocrine data are available in patients 7 to 10 in ←**Table 1**.[1] Serum testosterone was sufficiently high during the mini-puberty period, and response was well to human chorionic gonadotropin (hCG) stimulation during infancy to early childhood. This implies that *MAMLD1* mutations exert their deleterious effects primarily in the fetal period, as supported by the *Mamld1* expression pattern in the fetal and postnatal testes (see below). However, our long-term follow-up examinations have revealed that patients with *MAMLD1* mutations exhibit primary gonadal dysfunction in late childhood (our unpublished observation). This is consistent with weak but detectable *Mamld1* expression in the postnatal testis (our unpublished observation), and suggests deterioration in testicular function with age.

Expression Patterns of *MAMLD1*/*Mamld1*

In the human, PCR-based screening for cDNA samples has revealed ubiquitous expression of *MAMLD1* including fetal testis, with two in-frame splice variants, a major form with exon 4 and a minor form without exon 4.[1] Furthermore, RT-PCR analysis using human fetal testis has shown clear and gradually increasing expression of *MAMLD1* during the second trimester.[15]

More detailed expression studies have been performed in the mouse.[1] In situ hybridization (ISH) analysis has shown that, in the fetal testis, *Mamld1* is weakly expressed in the internal region at E11.5, and clearly expressed in Sertoli cells and in a small number of Leydig cells at E12.5. At E14.5, *Mamld1* is still clearly expressed in Sertoli cells and in the

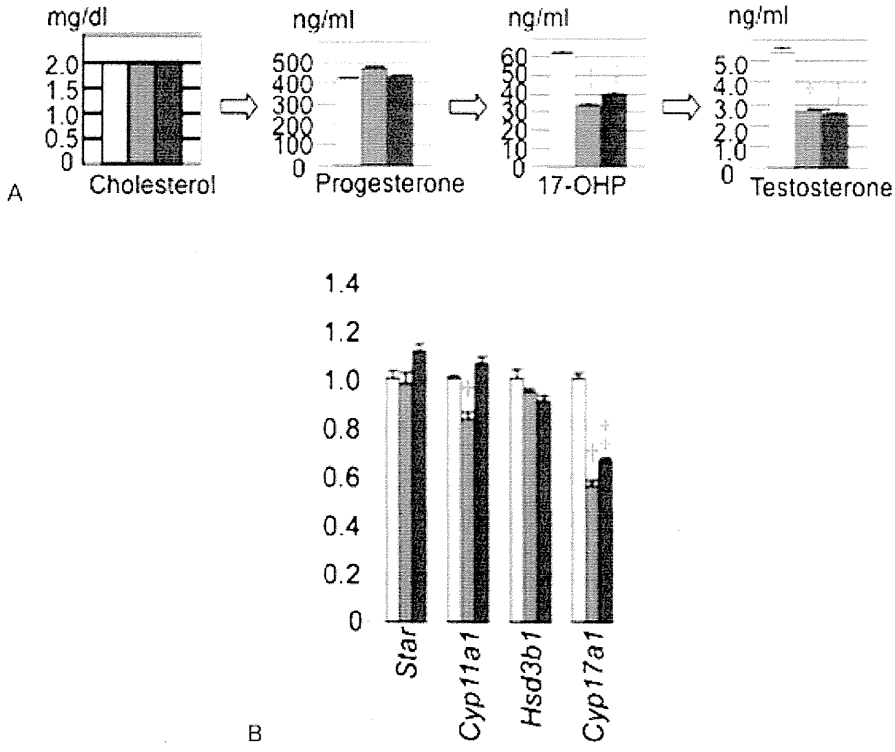

Figure 3 Representative data of the *Mamld1* knockdown experiments using MLTCs. Endogenous *Mamld1* expression has been markedly reduced to 10–15% by knockdown with si-RNAs. Shown are steroid metabolite concentrations in culture media and endogenous *Mamld1* expression levels in MLTCs. The white bars indicate the data obtained from MLTCs transfected with non-targeting RNA, and the light gray and the dark gray bars indicate the data obtained from MLTCs transfected with two different siRNAs.†: $P < 0.01$; and ‡: $P < 0.001$. (1) Representative steroid metabolite concentrations in culture media. (2) Real-time RT-PCR analysis for steroidogenic enzymes.

majority of Leydig cells. Such cell-type specific expression patterns were confirmed by co-localization of *Mamld1* mRNA and Nr5a1 (alias, steroidogenic factor 1 [SF1] or Ad4bp) protein as the marker for Sertoli and Leydig cells.[16,17] In the fetal ovary, *Mamld1* is expressed in a small number of somatic cells primarily at the boundary to the mesonephros at E11.5 and E12.5, and weakly expressed in a small number of somatic cells in the internal region at E14.5. In extragonadal tissues at E12.5, *Mamld1* is clearly expressed in the Müllerian ducts, forebrain, somite, neural tube, and pancreas, and weakly expressed in the external genital region. However, *Mamld1* expression is absent in the adrenals.

ISH analysis has revealed that, in the postnatal testis, *Mamld1* expression is weakly identified within the cords until one week of age and becomes faint thereafter; however, RT-PCT analysis still detects clear expression of *Mamld1* in the postnatal testis (our unpublished observation). In the ovary, *Mamld1* expression is barely detected until 2 weeks of age and clearly identified in granulosa cells at the perifollicular regions of most of Graafian follicles at 3 and 8 weeks of age.

Relevance of *Mamld1* to Testosterone Production

The above data imply that MAMLD1 is involved in the testosterone production in the critical period for sex development during fetal life, and that *MAMLD1* deletions/mutations cause hypospadias primarily because of compromised testosterone production around the critical period for sex development. In this context, there are two major possibilities how *MAMLD1* mutations lead to compromised testosterone production: (1) compromised steroidogenic activity in Leydig cells; and (2) reduced proliferation of Leydig cells. To test which of the two possibilities is more relevant, we performed knockdown analysis with two different siRNAs for *Mamld1*, using mouse Leydig tumor cells (MLTCs).[18] MLTCs are known to have the capacity to produce testosterone primarily via Δ^4-pathway, although the amount of testosterone production remains small primarily because of low 17α-hydroxylase and Hsd17b3 activities.[19] MLTCs are also known to retain responsiveness to hCG.[19–21]

Representative data of the steroidogenic activity are shown in ►**Fig. 3**; the data were obtained at 48 hours after the incubation of siRNA-transfected and non-transfected MLTCs followed by stimulation with hCG (for details, see reference[18]). The concentrations of pregnenolone and progesterone remained comparable between the culture media with siRNA-transfected MLTCs and those with nontargeted MLTCs, whereas the concentrations of 17-OH pregnenolone, 17-OH progesterone, dehydroepiandrosterone, androstenedione, and testosterone were significantly lower (~50–60%) in the culture media with siRNA-transfected MLTCs than in those with non-targeted MLTCs. Furthermore, comparison of

the steroid metabolite concentrations in the media with non-targeted MLTCs confirmed the Δ^4-pathway dominant testosterone production, markedly low 17α-hydroxylase activity and well-preserved 17/20 lyase activity for both Δ^4- and Δ^5-pathways, and extremely low Hsd17b3 activity in MLTCs. These results indicated that *Mamld1* knockdown further reduced 17α-hydroxylase activity that was originally low in MLTCs. Consistent with these findings, real-time RT-PCR and microarray analyses showed significantly decreased *Cyp17a1* expression (~70%) in siRNA-transfected MLTCs. The siRNAs knockdown did not affect the expressions of *Nr5a1* (Sf1), *Star*, *Por*, and *Insl3*. The assessment of *Hsb17b3* was impossible because of its extremely low expression. By contrast, the proliferation capacity, which was examined for 120 hours, was comparable between siRNA-transfected MLTCs and non-transfected MLTCs.

These results imply that *MAMLD1* is involved in testosterone production via augmenting CYP17A1 (17α-hydroxylase) activity. In this regard, it is noteworthy that *Mamld1* is clearly expressed in fetal Leydig and Sertoli cells and is barely expressed in adrenal cells,[1,7] and that 17α-hydroxylase activity is indispensable for testosterone production in Leydig cells.[22] Thus, it appears likely that *Mamld1* enhances *Cyp17a1* expression primarily in Leydig cells, permitting the production of a sufficient amount of testosterone for male sex development. In addition, since the expressions of other genes involved in testosterone production and insulin-like 3 biosynthesis were not clearly affected in siRNA-transfected MLTCs,[18] this would argue against the possibility that *Mamld1* knockdown causes a global dysfunction of MLTCs, resulting in testosterone hyposecretion.

However, a straightforward explanation appears to be difficult between impaired 17α-hydroxylase activity and reduced *Cyp17a1* expression. Indeed, 17/20 lyase activity was well preserved in siRNA-transfected MLTCs, although the same Cyp17a1 enzyme is utilized for both17α-hydroxylase and 17/20 lyase reactions.[22] In addition, defective 17α-hydroxylase activity occurred in the presence of ~70% of *Cyp17a1* expression, despite 17α-hydroxylase deficiency being an autosomal recessive disease in which 50% of enzyme reduction has no major effect on the steroid metabolism.[22] In this context, it is notable that MLTCs originally have a markedly low 17α-hydroxylase activity and a well preserved 17/20 lyase activity for both Δ^4- and Δ^5-pathways.[19] Such a unique property of MLTCs may be relevant to the preferential impairment of 17α-hydroxylase activity in siRNA-transfected MLTCs. Thus, although the in vitro data strongly argue for a positive role of *MAMLD1* in testosterone production, further studies are necessary to examine the precise in vivo function of *MAMLD1*.

Transcriptional Regulation of *MAMLD1*/*Mamld1* by *NR5A1*/*Nr5a1*

Mouse *Mamld1* is coexpressed with *Nr5a1* (Sf1), and *NR5A1*/*Nr5a1* is known to regulate the transcription of a vast array of genes involved in sex development, by binding to specific DNA sequences.[16,17] This implies that *MAMLD1*/*Mamld1* is also controlled by *NR5A1*/*Nr5a1*. Consistent with this notion, human *MAMLD1* harbors a putative NR5A1 binding sequence "CCAAGGTCA" at intron 2 upstream of the coding region, and mouse *Mamld1* also carries a putative Nr5a1 binding site at intron 1 upstream of the coding region.[9] Furthermore, we performed DNA binding and luciferase assays, showing that NR5A1 protein binds to the putative target sequence and exerts a transactivation function.[9] These findings argue for the possibility that *MAMLD1*/*Mamld1* expression is regulated by *NR5A1*/*Nr5a1*.

In Vitro Function of MAMLD1 Protein

MAMLD1 protein has a unique structure with homology to that of mastermind like 2 (MAML2) protein (**►Fig. 1**).[9] In particular, both MAMLD1 and MAML2 contain a unique amino acid sequence to which we designate mastermind-like (MAML) motif. The MAML motif was well conserved among MAMLD1 orthologs identified in frog, bird, and mammals. In addition, glutamine-, proline-, and serine-rich domains reside on MAMLD1.

MAML2 is a non-DNA binding transcriptional co-activator in Notch signaling that plays an important role in cell differentiation in multiple tissues by exerting either inductive or inhibiting effects according to the context of the cells.[23–25] Upon ligand-receptor interaction, Notch intracellular domain (N-ICD) is translocated from the cell surface to the nucleus and interacts with a DNA-binding transcription factor, recombination signal binding protein-J (RBP-J), to activate target genes like hairy/enhancer of split 1 (*Hes1*) and *Hes5*.[26] In this canonical Notch signaling process, MAML2 forms a ternary complex with N-ICD and RBP-J at nuclear bodies, enhancing the transcription of the Notch target genes.[23,24,27–29] In addition to such canonical Notch target genes, recent studies have shown that *Hes3* can be induced by stimulation with a Notch ligand, via a STAT3 mediated pathway.[30] This finding, together with lack of *Hes3* induction by N-ICD,[25] implies that *Hes3* represents a target gene of a non-canonical Notch signaling.

Thus, we have performed functional studies of wildtype MAMLD1 in terms of Notch signaling, thereby revealing several findings.[9] First, MAMLD1 is distributed in a speckled pattern and co-localized with the MAML2 protein in the nuclear bodies. Second MAMLD1, as well as MAML2, is unlikely to have a DNA-binding capacity. Third, although MAMLD1 is incapable of enhancing the promoter activities of the canonical Notch target genes *Hes1* and *Hes5* with the RBP-J binding site, MAMLD1 transactivates the promoter activity of the non-canonical Notch target gene *Hes3* without the RBP-J binding site. These findings imply that MAML2 and MAMLD1 may have derived from a common ancestor and evolved as a co-activator for the canonical and the non-canonical Notch signaling.

We have also performed similar functional studies for the three nonsense mutants identified in patients 7 to 10 (p.E124X, p.Q197X, and p.R653X) and missense variants (p.P286S, p.Q507R, and p.N589S).[9] The p.E124X and p.Q197X proteins, though they localize to the nucleus, are incapable of

localizing to nuclear bodies and have no transactivation function for Hes3, whereas the p.R653X protein as well as the three variant proteins localize to the nuclear bodies and retained nearly normal transactivating activities. This suggests that the p.E124X and p.Q197X proteins have no transactivation function primarily because of the failure in localizing to the nuclear bodies, and that the p.R653X protein, when it is artificially produced, has a normal transactivating activity. Thus, if not all the mRNAs with nonsense mutations are subject to NMD,[8] this would permit the production of functional protein for p.R653X, but not for p.E124X and p.Q197X. In addition, the transactivation function has been shown to be significantly reduced in a p.L103P protein (an artificially constructed variant affecting the MAML motif) and normal in the ΔExon 4.[9] This implies the importance of the MAML motif, and the biological equivalence between exon 4 positive and negative *MAMLD1*.

MAMLD1 Variations as a Susceptibility Factor for Hypospadias

It is possible that single nucleotide polymorphisms (SNPs), especially those in the promoter region and the cDNA sequence (cSNPs), and haplotypes (a combination of SNPs) of disease-causing genes constitute susceptibility factors of the corresponding diseases. In this regard, *MAMLD1* harbors several cSNPs, and the p.P286S and p.N589S cSNPs are fairly common in Caucasian populations, although they remain rare in the Japanese population.[1,12] In this regard, Chen et al[12] have revealed that the p.P286S allele, the p.N589S allele, and the p.P286S–p.N 589S haplotype (S–S haplotype) are more frequent in patients with hypospadias than in control males. While functional studies using the non-canonical Notch target Hes3 showed normal transactivation function for p.P286S allele, the p.N589S allele, and the 286S–589S haplotype (←**Fig. 2**), it is known that a substitution exerts differential effects on different promoters.[31] Thus, it remains possible that a specific SNP(s) or haplotype(s) may form a susceptibility factor for the development of hypospadias and other forms of 46,XY DSD.

Implications for Primary Ovarian Insufficiency

MAMLD1 may also have a certain role in the ovarian development. This notion is primarily based on two findings: (1) murine *Mamld1* is clearly identified in granulosa cells at the perifollicular regions of most of Graafian follicles at 3 and 8 weeks of age; and (2) a female with a heterozygous microdeletion involving *MAMLD1*, who gave birth to a boy with the same microdeletion and 46,XY DSD, has exhibited ovarian dysfunction from her late teens,[10] although ovarian dysfunction has not been identified in other obligatory carrier females. These findings may suggest that *MAMLD1* is involved in the normal ovarian development, and that rather exceptional females with a heterozygous *MAMLD1* mutation/deletion and skewered inactivation of the X chromosome carrying the normal allele manifest primary ovarian dysfunction. In this context, we examined a total of 78 females with primary ovarian insufficiency and 46,XX karyotype, and identified p.P494S and p.428delQ (shortening of the first polyglutamine domain from 11 to 10) (our unpublished observation). However, functional studies using Hes3 system showed apparently normal transcription activities for the two variants. Thus, further studies are necessary to reveal the relevance of *MAMLD1* to ovarian development.

Conclusions

MAMLD1 is a causative gene for 46,XY DSD with hypospadias as the salient clinical phenotype. It appears to play a supportive role in the testosterone production around the critical period for sex development. Interestingly, *Mamld1* knockout mice exhibit normal genital findings and reproductive functions, although they manifest metabolic syndrome (our unpublished observation). Further studies will permit to reveal the frequency of *MAMLD1* mutations in 46,XY DSD and the in vivo function of *MAMLD1*.

Acknowledgments

This study was supported in part by Grant for Research on Intractable Diseases (H22–098) from the Ministry of Health, Labor and Welfare, and by Grant-in-Aid for Scientific Research (S) (22227002) from the Japan Society for the Promotion of Science (JSPS), and by Grant-in-Aid for Scientific Research on Innovative Areas (22132004) from the Ministry of Education, Culture, Sports, Science and Technology (MEXT).

References

1 Fukami M, Wada Y, Miyabayashi K, et al. CXorf6 is a causative gene for hypospadias. Nat Genet 2006;38(12):1369–1371
2 Hu LJ, Laporte J, Kress W, et al. Deletions in Xq28 in two boys with myotubular myopathy and abnormal genital development define a new contiguous gene syndrome in a 430 kb region. Hum Mol Genet 1996;5(1):139–143
3 Laporte J, Guiraud-Chaumeil C, Vincent MC, et al; ENMC International Consortium on Myotubular Myopathy. European Neuro-Muscular Center. Mutations in the MTM1 gene implicated in X-linked myotubular myopathy. Hum Mol Genet 1997;6(9):1505–1511
4 Bartsch O, Kress W, Wagner A, Seemanova E. The novel contiguous gene syndrome of myotubular myopathy (MTM1), male hypogenitalism and deletion in Xq28:report of the first familial case. Cytogenet Cell Genet 1999;85(3–4):310–314
5 Biancalana V, Caron O, Gallati S, et al. Characterisation of mutations in 77 patients with X-linked myotubular myopathy, including a family with a very mild phenotype. Hum Genet 2003;112 (2):135–142
6 Laporte J, Kioschis P, Hu LJ, et al. Cloning and characterization of an alternatively spliced gene in proximal Xq28 deleted in two patients with intersexual genitalia and myotubular myopathy. Genomics 1997;41(3):458–462
7 Ogata T, Laporte J, Fukami M. MAMLD1 (CXorf6): a new gene involved in hypospadias. Horm Res 2009;71(5):245–252
8 Kuzmiak HA, Maquat LE. Applying nonsense-mediated mRNA decay research to the clinic: progress and challenges. Trends Mol Med 2006;12(7):306–316

9 Fukami M, Wada Y, Okada M, et al. Mastermind-like domain-containing 1 (MAMLD1 or CXorf6) transactivates the Hes3 promoter, augments testosterone production, and contains the SF1 target sequence. J Biol Chem 2008;283(9):5525–5532
10 Tsai TC, Horinouchi H, Noguchi S, et al. Characterization of MTM1 mutations in 31 Japanese families with myotubular myopathy, including a patient carrying 240 kb deletion in Xq28 without male hypogenitalism. Neuromuscul Disord 2005;15(3):245–252
11 Kalfa N, Liu B, Klein O, et al. Mutations of CXorf6 are associated with a range of severities of hypospadias. Eur J Endocrinol 2008;159(4):453–458
12 Chen Y, Thai HT, Lundin J, et al. Mutational study of the MAMLD1-gene in hypospadias. Eur J Med Genet 2010;53(3):122–126
13 Brandão MP, Costa EM, Fukami M, et al. MAMLD1 (mastermind-like domain containing 1) homozygous gain-of-function missense mutation causing 46,XX disorder of sex development in a virilized female. Adv Exp Med Biol 2011;707:129–131
14 Zitzmann M. The role of the CAG repeat androgen receptor polymorphism in andrology. Front Horm Res 2009;37:52–61
15 O'Shaughnessy PJ, Baker PJ, Monteiro A, Cassie S, Bhattacharya S, Fowler PA. Developmental changes in human fetal testicular cell numbers and messenger ribonucleic acid levels during the second trimester. J Clin Endocrinol Metab 2007;92(12):4792–4801
16 Morohashi KI, Omura T. Ad4BP/SF-1, a transcription factor essential for the transcription of steroidogenic cytochrome P450 genes and for the establishment of the reproductive function. FASEB J 1996;10(14):1569–1577
17 Parker KL, Schimmer BP. Steroidogenic factor 1: a key determinant of endocrine development and function. Endocr Rev 1997;18 (3):361–377
18 Nakamura M, Fukami M, Sugawa F, Miyado M, Nonomura K, Ogata T. Mamld1 knockdown reduces testosterone production and Cyp17a1 expression in mouse Leydig tumor cells. PLoS ONE 2011;6(4):e19123
19 Panesar NS, Chan KW, Ho CS. Mouse Leydig tumor cells produce C-19 steroids, including testosterone. Steroids 2003;68(3):245–251
20 Ascoli M, Puett D. Gonadotropin binding and stimulation of steroidogenesis in Leydig tumor cells. Proc Natl Acad Sci U S A 1978;75(1):99–102
21 Rebois RV. Establishment of gonadotropin-responsive murine leydig tumor cell line. J Cell Biol 1982;94(1):70–76
22 Achermann JC, Hughes IA. Disorders of sex development. In: Kronenberg HM, Melmed M, Polonsky KS, Larsen PR, eds. Williams textbook of endocrinology. 11th editions. Philadelphia: Saunders; 2008:783–848
23 Lin SE, Oyama T, Nagase T, Harigaya K, Kitagawa M. Identification of new human mastermind proteins defines a family that consists of positive regulators for notch signaling. J Biol Chem 2002;277 (52):50612–50620
24 Wu L, Sun T, Kobayashi K, Gao P, Griffin JD. Identification of a family of mastermind-like transcriptional coactivators for mammalian notch receptors. Mol Cell Biol 2002;22(21):7688–7700
25 Artavanis-Tsakonas S, Rand MD, Lake RJ. Notch signaling: cell fate control and signal integration in development. Science 1999;284 (5415):770–776
26 Iso T, Kedes L, Hamamori Y. HES and HERP families: multiple effectors of the Notch signaling pathway. J Cell Physiol 2003;194 (3):237–255
27 Nam Y, Sliz P, Song L, Aster JC, Blacklow SC. Structural basis for cooperativity in recruitment of MAML coactivators to Notch transcription complexes. Cell 2006;124(5):973–983
28 Wilson JJ, Kovall RA. Crystal structure of the CSL-Notch-Mastermind ternary complex bound to DNA. Cell 2006;124(5):985–996
29 Tonon G, Modi S, Wu L, et al. t(11;19)(q21;p13) translocation in mucoepidermoid carcinoma creates a novel fusion product that disrupts a Notch signaling pathway. Nat Genet 2003;33(2):208–213
30 Androutsellis-Theotokis A, Leker RR, Soldner F, et al. Notch signalling regulates stem cell numbers in vitro and in vivo. Nature 2006;442(7104):823–826
31 Ito M, Achermann JC, Jameson JL. A naturally occurring steroidogenic factor-1 mutation exhibits differential binding and activation of target genes. J Biol Chem 2000;275(41):31708–31714

NOTE

Advance Publication
doi: 10.1507/endocrj.EJ12-0257

Neuromuscular symptoms in a patient with familial pseudohypoparathyroidism type Ib diagnosed by methylation-specific multiplex ligation-dependent probe amplification

Keisuke Nagasaki[1), 2)*], Shuichi Tsuchiya[3)*], Akihiko Saitoh[2)], Tsutomu Ogata[1), 4)] and Maki Fukami[1)]

[1)] *Department of Molecular Endocrinology, National Research Institute for Child Health and Development, Tokyo 157-8535, Japan*
[2)] *Division of Pediatrics, Department of Homeostatic Regulation and Development, Niigata University Graduate School of Medical and Dental Sciences, Niigata 951-8510, Japan*
[3)] *Department of Pediatrics, Ojiya general Hospital, Niigata 947-8641, Japan*
[4)] *Department of Pediatrics, Hamamatsu University School of Medicine, Hamamatsu 431-3192, Japan*

Abstract. Pseudohypoparathyroidism type Ib (PHP-Ib) is a rare genetic disorder characterized by hypocalcemia and hyperphosphatemia due to imprinting defects in the maternally derived *GNAS* allele. Patients with PHP-Ib are usually identified by tetany, convulsions, and/or muscle cramps, whereas a substantial fraction of patients remain asymptomatic and are identified by familial studies. Although previous studies on patients with primary hypoparathyroidism have indicated that hypocalcemia can be associated with various neuromuscular abnormalities, such clinical features have been rarely described in patients with PHP-Ib. Here, we report a 12-year-old male patient with familial PHP-Ib and unique neuromuscular symptoms. The patient presented with general fatigue, steppage gait, and myalgia. Physical examinations revealed muscular weakness and atrophies in the lower legs, a shortening of the bilateral Achilles' tendons and absence of deep tendon reflexes. Laboratory tests showed hypocalcemia, hyperphosphatemia, elevated serum intact PTH level, and impaired responses of urinary phosphate and cyclic AMP in an Ellsworth-Howard test, in addition to an elevated serum creatine kinase level. Clinical features of the patient were significantly improved after 1 month of treatment with alfacalcidol and calcium. Methylation-specific multiplex ligation-dependent probe amplification (MS-MLPA) and subsequent PCR analyses identified a methylation defect at exon A/B of *GNAS* and a microdeletion involving exons 4-6 of the *GNAS* neighboring gene *STX16* in the patient and in his asymptomatic brother. The results suggest that various neuromuscular features probably associated with hypocalcemia can be the first symptoms of PHP-Ib, and that MS-MLPA serves as a powerful tool for screening of GNAS abnormalities in patients with atypical manifestations.

Key words: PHP-Ib, Neuromuscular symptoms, Hypocalcemia, *STX16*, MS-MLPA

PSEUDOHYPOPARATHYROIDISM (PHP; MIM 103580) is a genetically heterogeneous condition characterized by hypocalcemia and hyperphosphatemia resulting from end-organ resistance to PTH [1]. PHP is classified into 2 subtypes, PHP-Ia and -Ib, according to the molecular causes and clinical features of the patients [1]. PHP-Ia results from loss-of-function mutations in the maternally derived *GNAS* gene that encodes the stimulatory G protein α-subunit [1]. Patients with PHP-Ia manifest multiple hormone resistance and characteristic physical stigmata such as short stature, obesity, round face, brachydactyly, subcutaneous ossification, and mild to moderate mental retardation, which are collectively referred to as Albright's hereditary osteodystrophy (AHO) [1, 2].

PHP-Ib is caused by imprinting defects of the maternally derived *GNAS* allele; patients with this condi-

Submitted Jul. 17, 2012; Accepted Oct. 14, 2012 as EJ12-0257
Released online in J-STAGE as advance publication Oct. 25, 2012
Correspondence to: Keisuke Nagasaki, Division of Pediatrics, Department of Homeostatic Regulation and Development, Niigata University Graduate School of Medical and Dental Sciences, Niigata, 951-8510, Japan. E-mail: nagasaki@med.niigata-u.ac.jp
Maki Fukami, Department of Molecular Endocrinology, National Research Institute for Child Health and Development, Tokyo 157-8535, Japan. E-mail: mfukami@nch.go.jp
* K.N. and S.T. contributed equally to this work.

tion show hypomethylation at one or more of the 4 differentially methylated regions (DMRs) of *GNAS* [3-7]. Genetic causes of PHP-Ib include cryptic deletions within the genes neighboring *GNAS*, *STX16* and *NESP55*, and epimutation of *GNAS* DMRs [4, 5]. Patients with PHP-Ib manifest PTH resistance without AHO [1]. These patients are usually identified by hypocalcemia-associated neuromuscular irritability, such as tetany, generalized convulsions, and/or muscle cramps, although a substantial fraction of the patients remain asymptomatic and are identified only by familial studies [6, 7].

Previous studies of patients with primary hypoparathyroidism have shown that hypocalcemia can be associated with various types of neuromuscular symptoms [8, 9]. However, such clinical features have been rarely described in patients with PHP-Ib [10]. Here, we report a Japanese patient with familial PHP-Ib due to an intragenic deletion of *STX16*, who presented with unique neuromuscular symptoms.

Methods

Case report

This male patient was born as the third child to non-consanguineous Japanese parents at 39 weeks of gestation, after an uncomplicated pregnancy and delivery. His birth weight was 3482 g (+1.1 SD) and length 50 cm (+0.7 SD). Neonatal screening tests were normal. His postnatal growth and development were uneventful.

From the age of 6 years, he had general fatigue. At 12 years of age, he was seen by a local doctor because of general fatigue, gait disturbance, and myalgia in the lower legs. He was suspected to have congenital myopathy, and was referred to our clinic for further investigation. His height and weight at the time of examination were 161.4 cm (+1.1 SD) and 42.4 kg (-0.2 SD), respectively. Physical examinations revealed muscular atrophies with weakness in the lower legs, a shortening of the bilateral Achilles' tendons and absence of deep tendon reflexes. He showed a high stepping gait with markedly reduced strength of dorsiflexors of the ankles. Sense of touch and temperature was normal. The Chvostek's sign was positive, while the Trousseau's sign was negative. He had neither AHO stigmata nor episodes of tetany or convulsions. Laboratory examinations revealed hypocalcemia, hyperphosphatemia, and an elevated serum intact PTH level, together with decreased urinary calcium excretions (Table 1). Serum creatine kinase (CK) level was markedly elevated. An Ellsworth-Howard test showed impaired responses of both urinary phosphaturic and cyclic AMP levels (Table 1). The TSH level was slightly elevated, while free T4 and gonadotropin levels were within the normal range. The serum 1,25-dihydroxy vitamin D (1,25(OH)2D) level was mildly elevated. Head computerized tomography (CT) delineated symmetric calcifications of the basal ganglia and thalami, and subcortical calcification of the right middle frontal gyrus. Dual-energy X-ray absorptiometry (DEXA) revealed decreased bone mineral density at the lumbar spine (L2-L4) (0.640 g/cm^2, -2.9 SD). Based on these data, we diagnosed him as having PHP-Ib with neuromuscular symptoms. After 1 month of treatment with alfacalcidol (1.5 μg/day) and calcium lactate (3.0 g/day), his general fatigue, gait disturbance, and myalgia were markedly improved.

The 15-year-old brother of the patient manifested no clinically discernible phenotype; the brother had no gait disturbance or muscle weakness. Furthermore, physical examinations revealed neither muscular atrophy nor neurologic abnormalities. However, laboratory examinations detected an elevated serum intact PTH level, although serum calcium level was within the normal range (Table 1). Thus, the brother was also suspected as having PHP-Ib. The brother manifested mildly elevated serum 1,25(OH)2D level.

The 50-year-old father and 17-year-old sister were clinically normal. The mother, deceased at 49 years of age of an unknown cause, allegedly had no clinical symptoms indicative of PHP. Endocrine studies revealed no abnormalities in the father, sister, or mother (Table 1).

Molecular analyses

This study was approved by the Institutional Review Board Committee at the National Center for Child Health. After obtaining written informed consent, we extracted genomic DNA from leukocytes of the patient and his brother and father.

We examined mutations in the coding region of *GNAS* by direct sequencing, and copy number alternations and methylation defects in the *GNAS*-flanking region by methylation-specific multiplex ligation-dependent probe amplification (MS-MLPA), using a commercially available probe mix (SALSA MLPA kit, ME031-A1) (MRC-Holland, Amsterdam, The Netherlands). To confirm the results of MS-MLPA, we performed PCR analyses using forward and reverse

Table 1 Laboratory findings of the patient and his family members

	Patient	Brother	Father	Mother	Sister	Reference range
Age at the examinations (years)	12	15	50	43	17	
Height (cm) (SDS)	161.4 (+1.1)	171 (+0.1)	N.A.	N.A.	N.A.	
Weight (kg) (SDS)	42.4 (-0.2)	53 (-0.9)	N.A.	N.A.	N.A.	
<Blood>						
Intact PTH (pg/mL)	**430**	**254**	26	44	26	10-65
Calcium (mg/dL)	**6.4**	8.9	9.3	8.7	9.2	8.5-10.2
Phosphate (mg/dL)	**9.1**	**5.2**	2.9	3.8	3.4	2.4-4.3
Magnesium (mg/dL)	1.8	2.0	N.A.	N.A.	N.A.	1.8-2.5
Na (mEq/l)	142	140	N.A.	N.A.	N.A.	135-147
K (mEq/l)	4.1	4.0	N.A.	N.A.	N.A.	3.6-5.0
Creatinine (mg/dL)	0.6	0.7	N.A.	N.A.	N.A.	0.4-1.1
Alb (g/dL)	4.9	4.5	N.A.	N.A.	N.A.	3.9-5.1
CK (IU/L)	**741**	136	N.A.	N.A.	N.A.	0-170
ALP (IU/L)	**1809** (388-1190)[a]	648 (225-680)[a]	N.A.	N.A.	N.A.	
1,25(OH)2D (pg/mL)	**69**	**79**	N.A.	N.A.	N.A.	20-60
TSH (mU/L)	**5.6**	4.1	N.A.	N.A.	N.A.	0.5-5.0
Free T4 (ng/dL)	1.0	1.0	N.A.	N.A.	N.A.	0.9-1.6
<Urine>						
Calcium/Creatinine ratio	**0.004**	**0.008**	N.A.	N.A.	N.A.	0.08-0.20
%TRP	**99.6**	**99.6**	N.A.	N.A.	N.A.	89.6-93.6
<Ellsworth-Howard test>						
Urinary phosphate (mg/2 hrs)[b]	**8.33**	N.A.	N.A.	N.A.	N.A.	≥30
Urinary cAMP (μmol/hr)[c]	**0.029**	N.A.	N.A.	N.A.	N.A.	≥1.0

The conversion factors to the international system of units (SI unit) are as follows: intact PTH 1.0 (ng/liter), serum calcium 0.25 (mmol/liter), serum phosphate 0.3229 (mmol/liter) serum magensium 0.411 (mmol/liter), serum sodium 1.0 (mmol/liter), serum potassium 1.0 (mmol/liter), serum creatine 88.4 (μmol/liter), serum albumin 10 (g/liter), serum 1,25(OH_2)2D 2.6 (pmol/liter), serum Free T4 12.9 (pmol/liter). Hormone values have been evaluated by the age- and sex-matched Japanese reference data; abnormal data are in bold.

[a] The values in parentheses indicate the age-and sex-matched reference laboratory data.

[b] Urinary phosphate denotes the increment of 2 hours urinary excretion of phosphate after injection of human PTH (100 unit).

[c] Urinary cAMP denote the increment of 1 hour urinary cAMP excretion after injection of human PTH (100 unit).

N.A., not analysed; CK, creatine kinase; 1,25(OH)2D, 1,25-dihydroxy vitamin D; %TRP, % tubular reabsorption of phosphate

primers that hybridize to introns 3 and 6 of *STX16*, respectively [4].

Results

Direct sequence analysis for the patient identified no mutation in the coding region of *GNAS*. However, MS-MLPA revealed decreased peak heights of probes that correspond to exons 5 and 6 of *STX16*, indicating a heterozygous deletion within *STX16*. In addition, MS-MLPA indicated hypomethylation at *GNAS* exon A/B and a normal methylation pattern of the other 3 *GNAS* DMRs (Fig. 1A, B). Subsequent PCR analyses showed the presence of a heterozygous 3 kb deletion involving exons 4-6 of *STX16* (STX16Δexons 4-6) (Fig. 1C). The microdeletion and methylation defect were also observed in the brother, but not in the father. DNA samples of the mother and the sister were not available for genetic analyses.

Discussion

We report here a Japanese patient with PHP-Ib, who was identified by general fatigue, gait disturbance, and myalgia in the lower legs. He showed muscular atrophies in the lower legs, a shortening of the bilateral Achilles' tendons, absence of deep tendon reflexes, and an elevated serum CK value. Such clinical features are indicative of neuromuscular symptoms, although a detailed neurological workup was not performed for

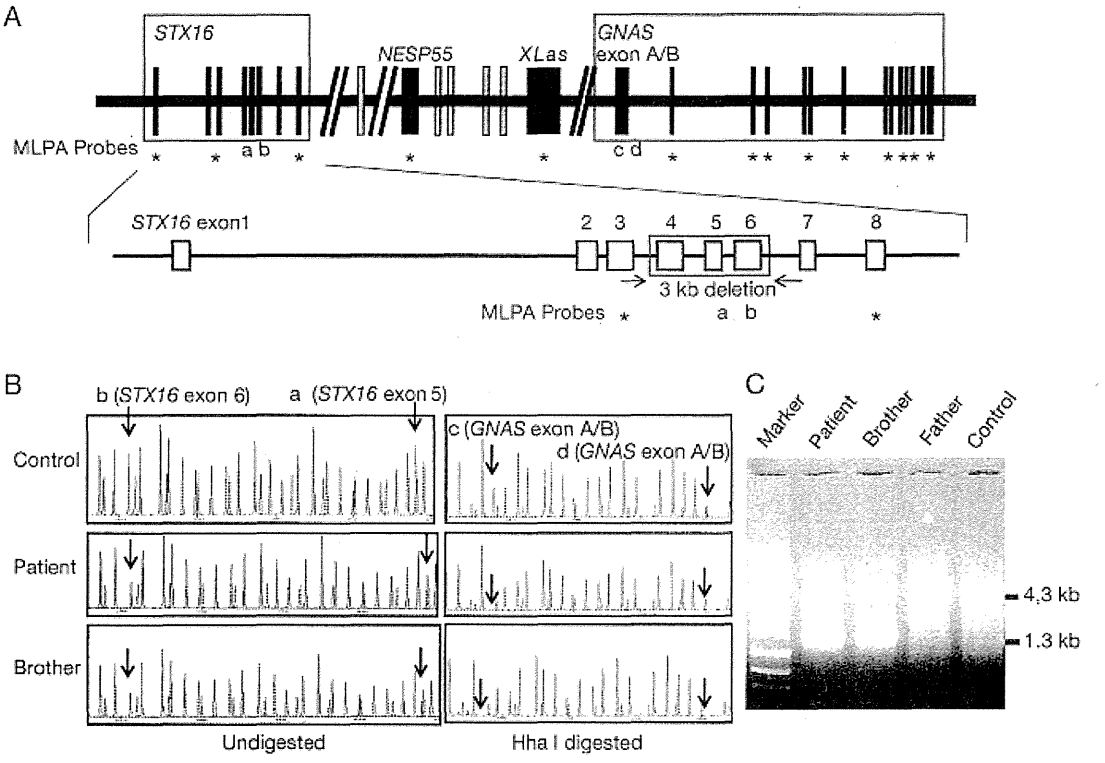

Fig. 1 Molecular analysis of the patient and his family members.
A, Schematic representation of the genomic region around *GNAS*. Upper panel: The loci examined by methylation-specific multiplex ligation-dependent probe amplification (MS-MLPA) are indicated by letters (a-d) and asterisks. Lower panel: Microdeletion identified in the patient and his brother. Horizontal arrows indicate the binding sites of the primers used for PCR analysis.
B. Representative results of MS-MLPA. Left panel: Decreased peak heights with probes a and b in the patient and his brother indicate heterozygous deletion involving exons 5 and 6 of *STX16*. Right panel: Absence of peaks with probes c and d indicate hypomethylation of *GNAS* exon A/B.
C, PCR analysis using a primer pair flanking the deletion. Both the 4.3 kb (wild-type) and 1.3 kb (STX16Δexons4-6) products were amplified from the patient and his brother, while only the 4.3 kb product was obtained from the father and the control individual.

this patient. In this regard, it is noteworthy that peripheral neuropathy and metabolic myopathy have been reported in patients with primary hypoparathyroidism [8, 9], whereas such symptoms have not been described in patients with PHP, except for mildly elevated blood CK and lactate dehydrogenase (LDH) levels in a single case of PHP-Ia [10]. Moreover, *in vitro* experiments showed that calcium concentration affects excitability at neuromuscular junctions [11]. Thus, the neuromuscular symptoms of our patient are likely to be associated with hypocalcemia. A significant improvement in the clinical features of the patient after 1 month of treatment with alfacalcidol and calcium supports this hypothesis. However, we cannot exclude the possibility that other factors such as vitamin D deficiency may also have played a role in the development of these features. Indeed, slightly elevated serum levels of ALP and 1,25(OH)2D in the patient are consistent with mild vitamin D deficiency [12]. On the other hand, since serum 1,25(OH)2D levels were similarly elevated in the patient and his asymptomatic brother, phenotypic variation in this family can not be explained by vitamin D deficiency. These results indicate that neuromuscular features probably associated with hypocalcemia can be the first symptoms of PHP-Ib. Nevertheless, this notion is based on observations of a single case, and

requires further investigations.

Both the patient and his brother carried a heterozygous STX16Δexons4-6. Although DNA samples of the mother were not available for genetic analyses, the absence of the deletion in the father indicated the maternal inheritance of the deletion. It has been shown that maternally inherited STX16Δexons4-6 (STX16Δexons4-6mat) is associated with hypomethylation at *GNAS* exon A/B, whereas *GNAS* epimutations are usually accompanied by methylation defects not only at exon A/B but also at other *GNAS* DMRs [3, 7]. These results suggest that the 3 kb region around exon 4-6 of *STX16* contains a cis-acting element that regulates methylation status at *GNAS* exon A/B. Consistent with this, our patient and his brother had methylation defects exclusively at exon A/B. Further studies are necessary to clarify the mechanism by which a DNA element >200 kb from *GNAS* controls the methylation status at exon A/B.

Clinical severities of patients with PHP-Ib are known to be variable [6, 7]. Notably, Linglart *et al.* have shown that STX16Δexons4-6mat is often associated with a mild phenotype. They found that about 40% of patients carrying this microdeletion remained asymptomatic, and more than 50% of asymptomatic individuals had normocalcemia at the time of diagnosis [7]. Consistent with this, our patient and his brother lacked typical PHP-Ib features such as tetany, generalized convulsions, or muscle cramps. Furthermore, the brother had normocalcemia. These results suggest that physical examinations and measurement of serum calcium levels are not sufficient to identify patients with PHP-Ib, and that genetic analyses or detailed endocrine evaluations, such as measurement of intact PTH levels and an Ellsworth-Howard test, are necessary for patients with atypical manifestations. In this context, although STX16Δexons4-6mat is the most frequent genetic cause of familial PHP-Ib [7], microdeletions affecting *NESP55* as well as epimutations of *GNAS* DMR also account for etiology of PHP-Ib [5, 7]. Since MS-MLPA is capable of detecting both copy number abnormalities and methylation defects in the *GNAS*-flanking region in a single assay, this method should be particularly useful for the molecular diagnosis of PHP-Ib.

In summary, the present study provides that various neuromuscular features probably associated with hypocalcemia can be the first symptoms of PHP-Ib, and suggests that MS-MLPA serves as a powerful tool for screening of *GNAS* abnormalities in patients with atypical manifestations.

Acknowledgments

We thank Dr. K. Kanno (Ojiya General Hospital) for providing us the blood samples of the family. We are also grateful to Ms. T. Tanji and E. Suzuki (National Research Institute for Child Health and Development) for their technical assistance, and Dr. J. Tohyama (Department of Pediatrics, Epilepsy Center, Nishi-Niigata Chuo National Hospital) for his fruitful discussion.

References

1. Levine MA (2000) Clinical spectrum and pathogenesis of pseudohypoparathyroidism. *Rev Endocr Metab Disord* 1: 265-274.
2. Weinstein LS, Yu S, Warner DR, Liu J (2001) Endocrine manifestations of stimulatory G protein alpha-subunit mutations and the role of genomic imprinting. *Endocr Rev* 22: 675-705.
3. Liu J, Litman D, Rosenberg MJ, Yu S, Biesecker LG, et al. (2000) A GNAS1 imprinting defect in pseudohypoparathyroidism type IB. *J Clin Invest* 106: 1167-1174.
4. Bastepe M, Frohlich LF, Hendy GN, Indridason OS, Josse RG, et al. (2003) Autosomal dominant pseudohypoparathyroidism type Ib is associated with a heterozygous microdeletion that likely disrupts a putative imprinting control element of GNAS. *J Clin Invest* 112: 1255-1263.
5. Bastepe M, Frohlich LF, Linglart A, Abu-Zahra HS, Tojo K, et al. (2005) Deletion of the NESP55 differentially methylated region causes loss of maternal GNAS imprints and pseudohypoparathyroidism type Ib. *Nat Genet* 37: 25-27.
6. Kinoshita K, Minagawa M, Takatani T, Takatani R, Ohashi M, et al. (2011) Establishment of diagnosis by bisulfite-treated methylation-specific PCR method and analysis of clinical characteristics of pseudohypoparathyroidism type 1b. *Endocr J* 58: 879-887.
7. Linglart A, Gensure RC, Olney RC, Juppner H, Bastepe M (2005) A novel STX16 deletion in autosomal dominant pseudohypoparathyroidism type Ib redefines the

boundaries of a cis-acting imprinting control element of GNAS. *Am J Hum Genet* 76: 804-814.
8. Kruse K, Scheunemann W, Baier W, Schaub J (1982) Hypocalcemic myopathy in idiopathic hypoparathyroidism. *Eur J Pediatr* 138: 280-282.
9. Goswami R, Bhatia M, Goyal R, Kochupillai N (2002) Reversible peripheral neuropathy in idiopathic hypoparathyroidism. *Acta Neurol Scand* 105: 128-131.
10. Piechowiak H, Grobner W, Kremer H, Pongratz D, Schaub J (1981) Pseudohypoparathyroidism and hypocalcemic "myopathy". A case report. *Klin Wochenschr* 59: 1195-1199.
11. Elmqvist D, Feldman DS (1965) Calcium dependence of spontaneous acetylcholine release at mammalian motor nerve terminals. *J Physiol* 181: 487-497.
12. Bringhurst FR, Demay MB, Kronenberg HM (2011) Hormones and disorders of mineral metabolism. In: Melmed S, Polonsky KS, Larson PR, Kronenberg HM (ed). Williams Textbook of endocrinology (12th). Saunders, Philadelphia: 1237-1304.

Pediatr Radiol (2012) 42:380–382
DOI 10.1007/s00247-011-2156-6

CASE REPORT

A case of Sjögren-Larsson syndrome with minimal MR imaging findings facilitated by proton spectroscopy

Yasuhiko Tachibana · Noriko Aida · Keisuke Enomoto · Mizue Iai · Kenji Kurosawa

Received: 7 March 2011 / Revised: 2 May 2011 / Accepted: 6 May 2011 / Published online: 29 June 2011

Abstract We present a 5-year-old girl who was ultimately diagnosed with Sjögren-Larsson syndrome (SLS). Although her MRI findings were minimal compared to previously published cases, prominent and characteristic abnormal lipid peaks on single-voxel proton MR spectroscopy (^{1}H-MRS) facilitated the diagnosis. This case emphasizes the importance and usefulness of ^{1}H-MRS in diagnosing SLS.

Keywords Sjögren-Larsson syndrome · MR spectroscopy · Lipids · Molecular study

Introduction

Sjögren-Larsson syndrome (SLS) is a rare autosomal-recessive neurocutaneous disorder characterized by a clinical triad of congenital ichthyosis, spastic diplegia or tetraplegia and mental retardation. The symptoms may be apparent at birth, and the syndrome usually develops in the first years of life [1]. The severity of the symptoms is variable and a few cases have very mild symptoms [2]; however, some hyperkeratosis seems inevitable. SLS is caused by deficiency of the microsomal enzyme fatty aldehyde dehydrogenase (FALDH) due to mutations in the *ALDH3A2* gene [3]. This results in accumulation of fatty alcohols, modification of macromolecules by fatty aldehydes and the presence of high concentrations of biologically active lipids, which have been postulated to be the pathophysiological mechanism of symptoms in SLS [1]. Previous studies regarding proton MR spectroscopy (^{1}H-MRS) of the brain in SLS patients have revealed abnormal lipid peaks at 1.3 ppm and/or 0.9 ppm [1], in addition to the characteristic MRI findings including a zone of abnormal high signal intensity in the periventricular white matter on T2-weighted images and delayed myelination development [1].

We present a girl with SLS whose brain MRI findings were minimal and nonspecific but who had prominent lipid peaks on ^{1}H-MRS. The suspicion of SLS was facilitated by this finding on ^{1}H-MRS in addition to her clinical symptoms. A distinct diagnosis based on a molecular analysis of her *ALDH3A2* gene was made.

Case report

The girl, born at 39 weeks' gestation to unrelated healthy parents, was 5 years old when she underwent MRI/^{1}H-MRS examination to evaluate unexplained lower limb spasticity. Her skin was normal in her first months of life, but hyperkeratosis on her trunk and limbs appeared in her first year of life, and developed into acanthosis and ichthyosis in the next year. However, SLS was not considered at the time. Her motor development was mildly delayed, with her achieving head control at 4 months, rolling over at 6 months, crawling at 12 months and walking without support at 21 months of age. She had a spastic gait with

Y. Tachibana (✉) · N. Aida
Department of Radiology, Kanagawa Children's Medical Center,
2-138-4 Mutsukawa, Minami-ku,
Yokohama, 232-8555, Japan
e-mail: yaz.tachibana@radio.email.ne.jp

K. Enomoto · K. Kurosawa
Division of Medical Genetics,
Kanagawa Children's Medical Center,
Yokohama, Japan

M. Iai
Department of Neurology, Kanagawa Children's Medical Center,
Yokohama, Japan

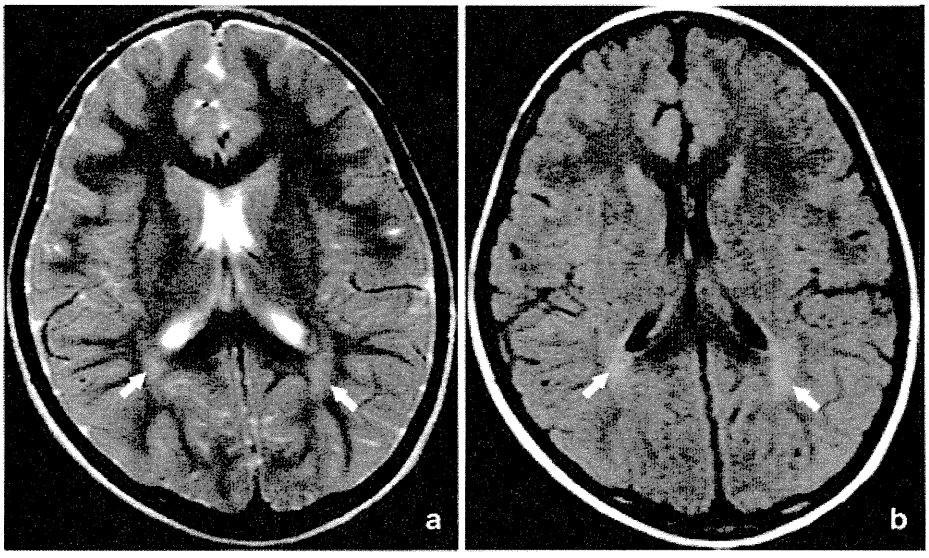

Fig. 1 MRI findings. **a** T2-weighted image (TR/TE=3,880/119 msec) and (**b**) T2-weighted fluid-attenuated inversion recovery image (TR/TE/TI=9,000/116/2,406 msec). The minimal high-intensity lesions in the deep white matter around the trigones of the bilateral lateral ventricles are scarcely distinguishable from a normal nonmyelinated lesion considering her age (*arrows*). TR = repetition time, TE = echo time, TI = inversion time

brisk deep tendon reflexes in her bilateral lower limbs, and developed worsening spasticity during her first 2 years. She had no deficiencies in intellectual development.

MR examinations were performed on a 1.5-T MRI system (Siemens MAGNETOM Avanto, Siemens Medical Solutions, Erlangen, Germany), by using a 12-channel head coil. ^{1}H-MRS was added to the MRI brain imaging sequences (i.e. transverse and sagittal T1-weighted spin-echo imaging, transverse and coronal T2-weighted fast spin-echo imaging, transverse diffusion-weighted imaging, and T2-weighted fluid-attenuated inversion recovery imaging (FLAIR), as is routinely done at our clinics when patients have neurological findings as in this case. ^{1}H-MRS was acquired by the single-voxel point resolved spectroscopy (PRESS) sequence. Repetition time (TR), echo time (TE) and the number of excitations (NEX) was set to 5,000 msec, 30 msec and 6, respectively. The volume of interest was set to the left centrum-semiovale (where no MRI abnormality was seen), which measured 40 mm× 25 mm×25 mm (Fig. 2). To note, another ^{1}H-MRS with longer TE (TR/TE/NEX set to 5,000 msec/135 msec/15) was acquired at the same volume of interest in addition (Fig. 2), as described later.

T2-weighted images and FLAIR images demonstrated slight minimum high-intensity areas around the trigones of the bilateral lateral ventricles, which were hardly distinguishable from the terminal zone (Fig. 1). No other pathological finding was noted in the MRI examination. On the other hand, ^{1}H-MRS revealed a prominent and narrow abnormal peak at 1.3 ppm and a relatively small narrow peak at 0.9 ppm (Fig. 2). To exclude lactate from the peak at 1.3 ppm, the aforementioned additional ^{1}H-MRS with longer TE was acquired at the same volume of interest. The peaks at 1.3 ppm and 0.9 ppm remained at this setting (Fig. 2), suggesting that they were derived from lipids, as the peak at 1.3 ppm would have been inverted if it

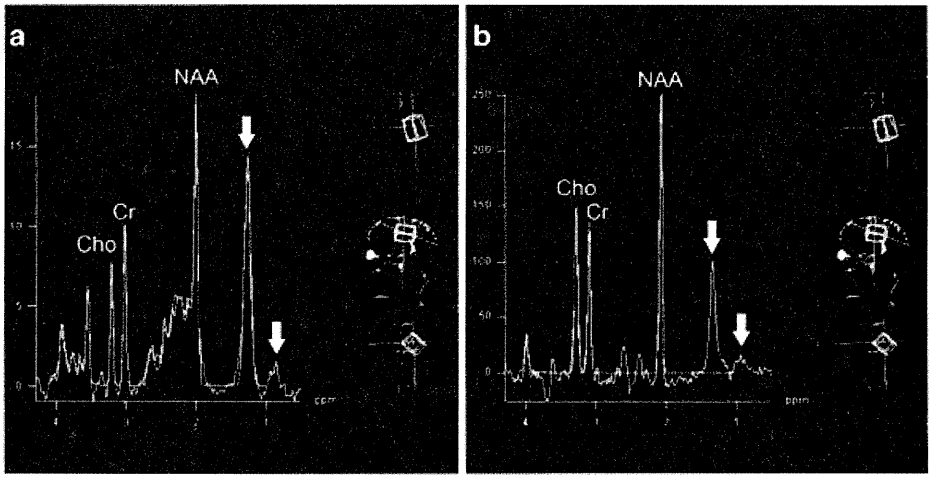

Fig. 2 MR spectroscopy. **a** Proton MR spectroscopy (^{1}H-MRS) (TR/TE/NEX=5,000 msec/30 msec/6) and (**b**) ^{1}H-MRS (TR/TE/NEX=5,000 msec/135 msec/15) both acquired at the same volume of interest at the left centrum-semiovale. Narrow abnormal resonance peaks at 1.3 ppm and 0.9 ppm are demonstrated in both (**a**) and (**b**) (*arrows*). NEX = number of excitations. *NAA* = N-acetyl aspartate. *Cr* = creatine. *Cho* = choline

were derived from lactate. A quantitative analysis based on LCModel was made and lipid peak at 1.3 ppm was confirmed. Other major molecules, including N-acetylaspartate, creatine, myo-inositol and choline, which were all within normal limits, were also confirmed on LCModel. Based on the ^{1}H-MRS finding, in addition to the clinical symptoms, molecular analysis was conducted for suspicion of SLS.

Molecular analysis

Written informed consent was obtained from the girl's parents. Sequencing of all 11 exons and exon/intron junctions of the ALDH3A2 gene identified two mutations including c.1339A > G (p.K447E) in exon 9 and c.504_505insAG (p.Glu169ArgfsX8) in exon 4 in the heterozygote state, respectively. The first mutation is known as a disease-causing allele, resulting in reduced FALDH activity as low as 1% of normal [4]. The final diagnosis of SLS was made. Of note, the second mutation is a novel mutation of ALDH3A2 not previously described.

Discussion

This case emphasizes the importance and usefulness of ^{1}H-MRS in diagnosing SLS, since the genetic testing was difficult to be triggered from the mild clinical symptoms and nonspecific MRI findings alone. It is well known that SLS is characterized by unusual narrow and prominent resonance peaks at 1.3 ppm and 0.9 ppm in ^{1}H-MRS, which correspond to the resonance of lipids. This finding is observed in all SLS cases published to date without exception when ^{1}H-MRS was acquired from the deep cerebral white matter of the brain [1, 5]. The MRI findings of the present case may be milder than any of the others. Another case of SLS reported by Nakayama et al. [5] also demonstrates mild MRI findings despite the prominent lipid peak on ^{1}H-MRS, but we presume that the MRI findings of our case are even less notable, especially given that ^{1}H-MRS in our case was acquired from a region without any MRI abnormalities, compared to the previous case that acquired ^{1}H-MRS from an area with abnormal high intensity in T2-weighted imaging. Willemsen et al. [1] evaluated ^{1}H-MRS acquired from 18 SLS patients and reported elevated levels of creatine (+14%), choline (+18%) and myo-inositol (+54%) in addition to lipids, but the molecules other than lipids were not elevated in our case.

The prominent and narrow resonance at 1.3 ppm is where the protons of methylene groups ($-[CH_2]_n-$) resonate, while the resonance at 0.9 ppm is where the protons of methyl groups ($-[CH_2]_n-CH_3$) resonate. These peaks in SLS presumably represent lipids that accumulate because of the FALDH deficiency, which may be fatty alcohols, fatty aldehydes and their metabolites [1]. It may be important to note that the resonance at 1.3 ppm and 0.9 ppm is not specific to SLS. Previous studies reported unusual peaks at 1.3 ppm (and 0.9 ppm) in other pathological states, including peroxisomal diseases such as Zellweger syndrome [6] or rhizomelic chondrodysplasia punctata [7], and other diseases including cerebrotendinous xanthomatosis [8]. In those cases, the lipid peaks are less prominent and broader compared to SLS, and visualized only in a short echo time (e.g., 30 msec) in contrast to SLS, in which peaks are visualized in a longer echo time (135 msec in the presented case). However, we still may not make a diagnosis of SLS based solely on a finding of these abnormal peaks on ^{1}H-MRS because methylene groups and methyl groups are both quite common structures in organic matters, and many other diseases (including metabolic and storage disorders of higher fatty acids and/or higher hydrocarbon) or conditions of destroyed normal tissue may present similar abnormal peaks.

In patients without typical clinical symptoms or without prominent white matter abnormality on MRI, ^{1}H-MRS is a useful tool to facilitate an appropriate molecular survey to make a diagnosis of SLS.

References

1. Willemsen MA, Van Der Graaf M, Van Der Knaap MS et al (2004) MR imaging and proton MR spectroscopic studies in Sjogren-Larsson syndrome: characterization of the leukoencephalopathy. AJNR 25:649–657
2. Ganemo A, Jagell S, Vahlquist A (2009) Sjogren-larsson syndrome: a study of clinical symptoms and dermatological treatment in 34 Swedish patients. Acta Derm Venereol 89:68–73
3. Rizzo WB (2007) Sjogren-Larsson syndrome: molecular genetics and biochemical pathogenesis of fatty aldehyde dehydrogenase deficiency. Mol Genet Metab 90:1–9
4. Rizzo WB, Carney G, Lin Z (1999) The molecular basis of Sjogren-Larsson syndrome: mutation analysis of the fatty aldehyde dehydrogenase gene. Am J Hum Genet 65:1547–1560
5. Nakayama M, Tavora DG, Alvim TC et al (2006) MRI and 1H-MRS findings of three patients with Sjogren-Larsson syndrome. Arq Neuropsiquiatr 64:398–401
6. Bruhn H, Kruse B, Korenke GC et al (1992) Proton NMR spectroscopy of cerebral metabolic alterations in infantile peroxisomal disorders. J Comput Assist Tomogr 16:335–344
7. Viola A, Confort-Gouny S, Ranjeva JP et al (2002) MR imaging and MR spectroscopy in rhizomelic chondrodysplasia punctata. AJNR 23:480–483
8. Embirucu EK, Otaduy MC, Taneja AK et al (2010) MR spectroscopy detects lipid peaks in cerebrotendinous xanthomatosis. AJNR 31:1347–1349

RESEARCH ARTICLE

AMERICAN JOURNAL OF medical genetics PART A

Clinical and Radiological Features of Japanese Patients With a Severe Phenotype due to *CASK* Mutations

Jun-ichi Takanashi,[1,2]* Nobuhiko Okamoto,[3] Yuto Yamamoto,[3] Shin Hayashi,[4] Hiroshi Arai,[5] Yukitoshi Takahashi,[6] Koichi Maruyama,[7] Seiji Mizuno,[7] Shuichi Shimakawa,[8] Hiroaki Ono,[9] Reiki Oyanagi,[10] Satomi Kubo,[11] A. James Barkovich,[12] and Johji Inazawa[4]

[1]Department of Pediatrics, Kameda Medical Center, Kamogawa, Japan

[2]Department of Radiology, Toho University Sakura Medical Center, Sakura, Japan

[3]Department of Medical Genetics, Osaka Medical Center and Research Institute for Maternal and Child Health, Osaka, Japan

[4]Department of Molecular Cytogenetics, Medical Research Institute and School of Biomedical Science, Tokyo Medical and Dental University, Tokyo, Japan

[5]Department of Pediatric Neurology, Morinomiya Hospital, Osaka, Japan

[6]National Epilepsy Center, Shizuoka Institute of Epilepsy and Neurological Disorders, Shizuoka, Japan

[7]Department of Pediatric Neurology, Aichi Prefectural Colony Central Hospital, Kasugai, Japan

[8]Department of Pediatrics, Osaka Medical College, Takatsuki, Japan

[9]Department of Pediatrics, Hiroshima Prefectural Hospital, Hiroshima, Japan

[10]Department of Pediatrics, Hokkaido Medical Center for Child Health and Rehabilitation, Sapporo, Japan

[11]Department of Pediatrics, Nara Prefectural Nara Hospital, Nara, Japan

[12]Department of Radiology and Biomedical Imaging, University of California San Francisco, California

Manuscript Received: 31 March 2012; Manuscript Accepted: 5 August 2012

Heterozygous loss of function mutations of *CASK* at Xp11.4 in females cause severe intellectual disability (ID) and microcephaly with pontine and cerebellar hypoplasia (MICPCH). However, the longitudinal clinical and radiological course of affected patients including patterns of postnatal growth has not been described. Neurodevelopmental and imaging information was retrospectively accrued for 16 Japanese (15 female and 1 male) patients with ID and MICPCH associated with *CASK* mutations. All records were analyzed; patient age ranged from 2 to 16 years at the time of the most recent examination. The growth pattern, neurological development, neurological signs, symptoms, and facial features were similar in the 15 female patients. Their head circumference at birth was within the normal range in about half, and their height and weight were frequently normal. This was followed by early development of severe microcephaly and postnatal growth retardation. The patients acquired head control almost normally between 4 and 6 months, followed by motor delay. More than half of the female patients had epilepsy. Their MRIs showed microcephaly, brainstem and cerebellar hypoplasia in early infancy, and a normal or large appearing corpus callosum. The male patient showed a more severe clinical phenotype. Documentation of clinical and radiological features should facilitate an early diagnosis and be useful for medical care of females with ID and MICPCH associated with *CASK* mutations.

How to Cite this Article:
Takanashi J-i, Okamoto N, Yamamoto Y, Hayashi S, Arai H, Takahashi Y, Maruyaa K, Mizuno S, Shimakawa S, Ono H, Oyanagi R, Kubo S, Barkovich AJ, Inazawa J. 2012. Clinical and radiological features of Japanese patients with a severe phenotype due to *CASK* mutations.
Am J Med Genet Part A 158A:3112–3118.

Grant sponsor: Research Grant for Nervous and Mental Disorders, Ministry of Health, Labor and Welfare of Japan; Grant number: 24-7; Grant sponsor: Grant-in-Aid for Scientific Research (C), JSPS; Grant number: 24591790; Grant sponsor: Health and Labor Sciences Research Grants, Ministry of Health, Labor and Welfare of Japan; Grant sponsor: New Energy and Industrial Technology Development Organization (NEDO).
The authors declared that they have no conflicts of interest.
*Correspondence to:
Jun-ichi Takanashi, Department of Pediatrics, Kameda Medical Center, 929 Higashi-cho, Kamogawa-shi, Chiba 296-8602, Japan.
E-mail: jtaka44@hotmail.co.jp
Article first published online in Wiley Online Library (wileyonlinelibrary.com): 19 November 2012
DOI 10.1002/ajmg.a.35640

Key words

INTRODUCTION

The CASK protein belongs to the membrane-associated guanylate kinase protein family, functioning as a multi-domain scaffolding protein, and plays important roles in neural development and synaptic function [Hsueh, 2006, 2009; Hayashi et al., 2008; Najm et al., 2008]. It has been reported that *CASK* aberrations can cause three clinical phenotypes, severe intellectual disability (ID) and microcephaly with pontine and cerebellar hypoplasia (MICPCH, OMIM: #300749) in females [Takanashi et al., 2010; Moog et al., 2011; Hayashi et al., 2012], mild to severe ID with or without nystagmus, microcephaly, and/or dysmorphic features in males [Hackett et al., 2010], and FG syndrome in males [Piluso et al., 2009] depending on the type of aberration of the gene [Moog et al., 2011; Hayashi et al., 2012]. Hypomorphic missense mutations of *CASK* in males probably cause FG syndrome or mild to severe ID with or without nystagmus, microcephaly, and/or dysmorphic features, whereas *CASK* null mutations (haploinsufficiency of *CASK*) in females cause ID and MICPCH [Moog et al., 2011; Hayashi et al., 2012]. This theory explains the similarity of the clinical and radiological phenotypes of ID and MICPCH regardless of the type of *CASK* mutation [Takanashi et al., 2010; Moog et al., 2011; Hayashi et al., 2012]; however, no long-term clinical and radiological information has been published on this group of patients. We present clinical and radiological evaluations of 16 Japanese patients with ID and MICPCH associated with *CASK* mutations.

MATERIALS AND METHODS

Sixteen Japanese patients (15 female and 1 male, 2–16 years old) clinically diagnosed with ID and MICPCH and confirmed to have *CASK* mutations were enrolled in this study. Written informed consent for genetic and clinical analysis was obtained from the parents after institutional review board approval was obtained from Tokyo Medical and Dental University and Kameda Medical Center. Genetic analysis and brief clinical features of 10 of the 16 patients [Hayashi et al., 2012], and magnetic resonance imaging (MRI) features of 5 of the 16 patients [Takanashi et al., 2010] were previously reported, respectively. The 15 female patients most likely have *CASK* loss-of-function mutations [Hayashi et al., 2012], which are expected to cause a characteristic pattern of ID and MICPCH in females [Moog et al., 2011; Hayashi et al., 2012]. In silico prediction programs and splice site prediction software showed that the de novo mutation in a male (Patient 16), situated in an important interaction domain of CASK, was considered to damaging to protein function, and this position was not associated with a splice site. We reviewed all available data, including MRI scans, raw data from the MRIs for use in quantification, and information concerning growth, development, and neurologic status. Height, weight, and head circumference were measured in all patients at birth, and subsequently recorded two to five times for female patients, and six times for the male. The MRI data with 1.5 T magnet were used to quantify the area of the cerebrum, cerebellar hemispheres, pons, and corpus callosum in each patient using the same methods previously reported [Takanashi et al., 2010]; patients ranged in age from 4 to 156 months at the time of their MRI. One (Patient 11) was scanned three times at ages 9, 24, and 50 months. The results of these measurements were compared with those of 62 female patients (0.5–180 months old) evaluated at the Kameda Medical Center using 1.5 T Siemens apparatus for mild neurological symptoms, such as headache, hypotonia, seizures, febrile delirium, or mild asphyxia, who had no parenchymal lesion on MRI, and showed normal subsequent neurodevelopmental exams; as well as those of five patients with pontine hypoplasia due to causes other than *CASK* mutations, including PEHO [Tanaka et al., 1997], 5p-syndrome [Ninchoji and Takanashi, 2010], and trisomy 18 (disease controls).

RESULTS

Clinical Records

The epilepsy and genetic data of the 16 patients with ID and MICPCH associated with *CASK* mutations are summarized in Table I. Postnatal growth curves are shown in Figure 1 (head circumference in Fig. 1a; height and weight in Fig. 1b,c). Fifteen patients were born at term (>37 weeks gestation); mean OFC was 30.4 ± 1.7 (mean $\pm$ SD) cm, height was 47.0 ± 2.6 cm, and weight was 2640 ± 420 g. Patient 5 was born at 33 weeks' gestation with an OFC of 28.0 cm, height of 41.4 cm, weight of 1596 g. Microcephaly, defined as less than the third centile (30.2 cm), was present at birth in 7/15 (47%) patients born at term. Microcephaly was recognized in all patients examined after age 4 months, with OFC measuring below −4 SD, including a male patient (Fig. 1, stars) and a female born at 33 weeks. Height at birth was low normal (within 2 SD) in 13/15 patients born at term, declining to around the −2 SD level after 4 years, and below the −3 SD level after 8 years. Birth weight was normal or low normal in 14/15 patients born at term, decreasing to the −1 SD to −2 SD level after 4 months, and around the −2 SD after 2 years. Height and weight of a male patient (Fig. 1, stars) and a female born at 33 weeks overlapped those of females born at term.

Hypotonia was observed in 11/16, muscle weakness in 10/16, spasticity or increased deep tendon reflexes in 12/16, involuntary movements in 3/16, sensory deafness in 2/16, and ophthalmologic anomalies in 3/16 (abnormal visual evoked potentials, strabismus, and nystagmus), respectively. Four patients presented with hypohidrosis, and two of these also showed hyposensitivity to pain. A typical facial appearance (Fig. 2) was noted (including the male patient, Fig. 2b), with an oval face in all patients, large eyes, or irises in 13/16, large ears in 11/16, a broad nasal bridge in 14/16, a broad nasal tip in 9/16, a small nose in 6/16, epicanthal folds in 5/16, a small jaw in 11/16, a long philtrum in 7/16, and a high-arched palate in 7/16.

The motor milestones are shown in Figure 3. The male (Patient 16) showed no psychomotor development at 5 years old, that is, he could not control his head, smile, or babble. The 15 female patients exhibited early psychomotor development; all

TABLE I. Features of Epilepsy in Patients With ID and MICPCH Associated With *CASK* Mutations.

Pt	Age (Mo)	M/F	Epilepsy/seizure type	Onset (Mo)	EEG	Therapy	Response	*CASK* mutation
1	190	F	GE/atonic	65	bil. F. and diffuse slow SWC	VPA, CZP, ESM	PR	Pt. No. in Hayashi et al. [2012]
2	42	F						c.2302 + delT
3	33	F	ES, CPS	17	bil. F. spikes			c.173_173 + 1gelGG
4	24	F				VPA, ACTH, TPM, LTG	Intractable	c.316C > G p.Arg106Stop
5	95	F	LGS/atonic, myoclonic, spasms	43	diffuse slow SWC			c.1910G > A p.Gly637Asp
6	147	F	CPS	17	left O. SWC	VPA, CLB, TPM, LTG	CR	del(X)(p11.3p11.4)
7	63	F			Normal	VPA, GBP	PR	9
8	111	F	FLE	60	bil. F. spikes			3
9	61	F				VPA, CBZ	CR	10
10	36	F	ES	34	Normal			1
11	49	F				VPA	CR	4
12	124	F	EMA	108	bil. F. SWC, bil. P.O. spikes			8
13	194	F	GE/tonic	130	left C.P., right C.P. spikes	VPA, CZP, ESM	Intractable	5
14	184	F			Normal	VPA	CR	7
15	27	F						6
16	63	M	WS, GE/tonic, myoclonic	4	4 Mo hyps, 5 years left F.C. spikes			2
						ACTH, VPA, PHT	Intractable	c.1061T > C p.Leu348Pro

Abbreviations: Pt, patient; M, male; F, female; Mo, month; GE, generalize epilepsy; ES, epileptic spasms; CPS, complex partial seizure; LGS, Lennox–Gastaut syndrome; FLE, frontal lobe epilepsy; EMA, epilepsy with myoclonic absences; WS; West syndrome; bil, bilateral; F, frontal; SWC, spike and wave complex; O, occipital; P, parietal; C, central; hyps, hypsarrhythmia; VPA valproate; CLB clobazam; TPM, topiramate; LTG, lamotrigine; GBP, gabapentin; CBZ, carbamazepine; ESM, ethosuximide; ACTH, adrenocorticotropic hormone; PHT, phenytoin; PR, partial remission, CR, complete remission.

could control their head at ages 3–6 (4.6 ± 1.2) months. Sitting independently was possible in 13/15 patients between 7 and 25 (14.2 ± 5.7) months, and walking independently in five between 29 and 72 months. All 15 female patients could smile, only four could babble, and one could utter a word.

The male patient presented with West syndrome (epileptic spasms and hypsarrhythmia) at 4 months, followed by generalized epilepsy, which was intractable to antiepileptic drugs. Eight of the 15 female patients (53%) had epilepsy, with onset between 17 and 130 (mean, 60) months, including two with epileptic spasms (no hypsarrhythmia), one with Lennox–Gastaut syndrome. EEG showed variable abnormalities, the most common finding being bilateral frontal spikes or spike and wave complexes in four patients. The response to antiepileptic drugs was also variable.

MRI Findings

The representative MRI (Fig. 4) and MRI measurements (areas of cerebrum, cerebellar hemispheres, pons, and corpus callosum), and the cerebrum/corpus callosum ratio of the controls and patients are shown in Figure 5. The areas of all measured regions increased with increasing age in the controls, whereas the cerebrum/corpus callosum ratio decreased with age, reaching the adult value at around age 5 years. In the CASK patients, the area of the cerebrum,

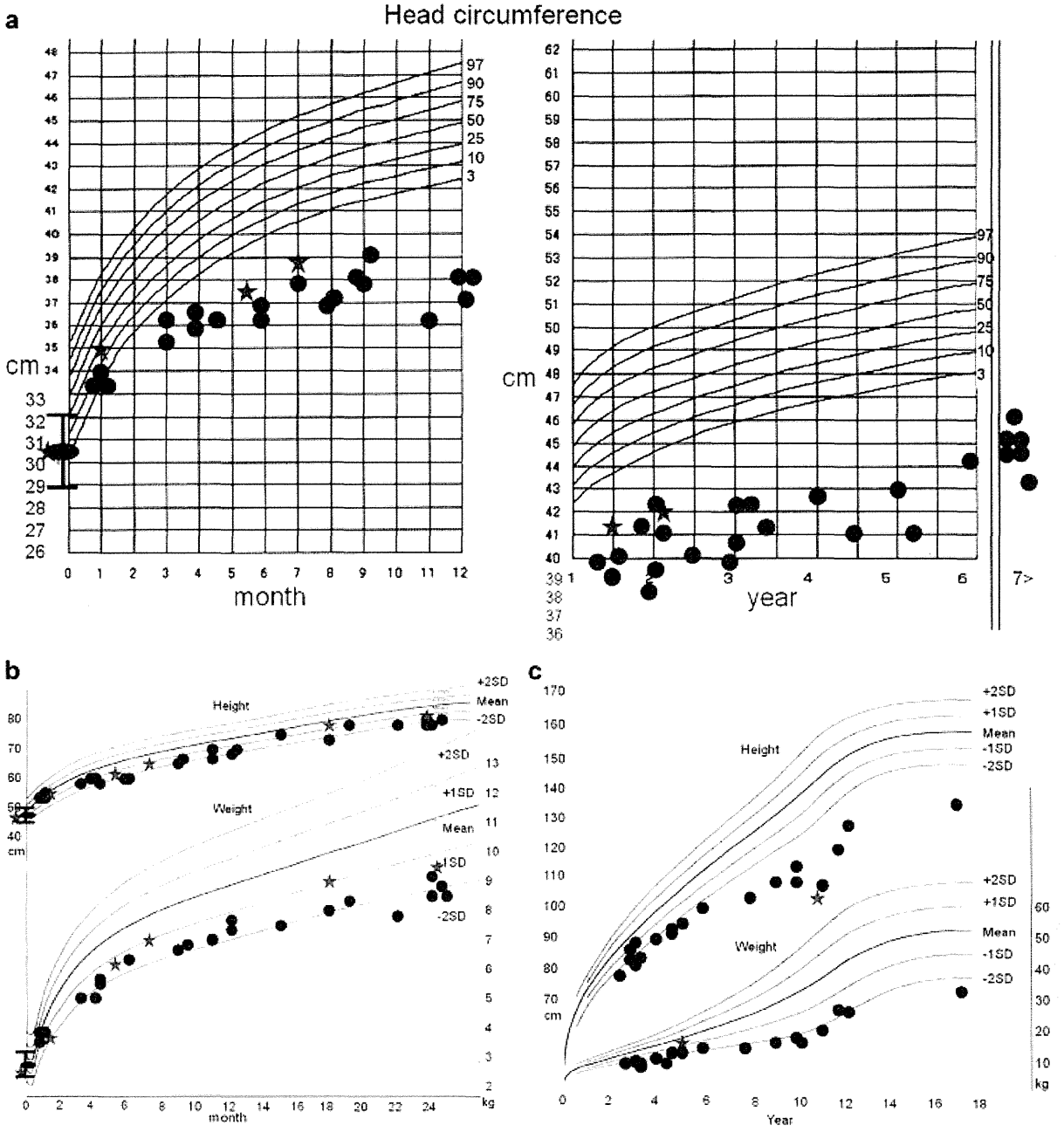

FIG. 1. Growth curves for head circumference (a), height, and weight (b,c). Black circles represent female patients, and stars a male patient. Large circle with bars represent mean ± standard deviation at birth.

cerebellar hemispheres, and pons (Fig. 5a–c) were much reduced in size when compared to controls, even in early infancy (after 4 months), and showed little size increase with age. The midline corpus callosum area was normal or in the low-normal range in all patients (Fig. 5d), appearing abnormally thick compared to the small cerebrum. The cerebellum/corpus callosum ratio was low normal or low in all patients with ID and MICPCH associated with *CASK* mutations (Fig. 5e). No obvious malformations were seen in the cerebral hemispheres in the 16 patients. In all five patients with non-*CASK*-related pontine hypoplasia, the corpus callosum was reduced in size and the cerebrum/corpus callosum ratio was high.

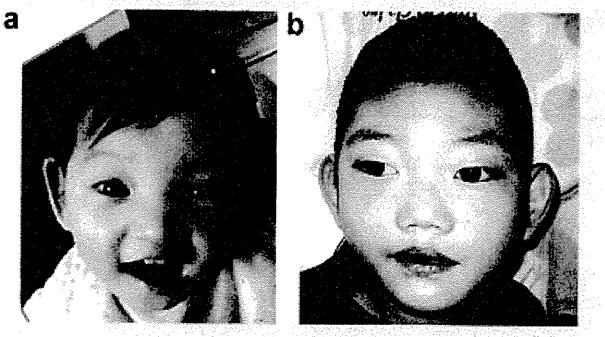

FIG. 2. Facial photograph of female Patient 11 (a) and male Patient 16 (b) showing an oval face, large eyes or irises, large ears, a broad nasal bridge, a broad nasal tip, and epicanthal folds.

DISCUSSION

This study revealed or confirmed several important clinical and radiological findings in Japanese patients with ID and MICPCH associated with *CASK* mutations. First, their head circumference at birth is within the normal range in about half, and birth height and weight are frequently normal; followed by postnatal growth retardation. Severe microcephaly develops usually within the first 4 months of life. Second, female patients acquire head control almost normally (between 3 and 6 months), but this is followed by motor delay. Third, more than half the female patients have epilepsy. In addition, MRI analyses showed that microcephaly and pontine and cerebellar hypoplasia develop in early infancy, and the corpus callosum is normal in size but appears large because the cerebrum is small. Finally, a male patient had a more severe clinical phenotype.

Microcephaly (−4 SD) and diminished body weight (−2 SD) became obvious after 4 months, while diminished stature (−2 to −3 SD) noted after 4 years. These findings are similar to those in a previous report of patients with *CASK* mutations in European countries [Moog et al., 2011]. MRI revealed that the area of the cerebrum is reduced in size after age 4 months, which was compatible with the OFC measurement. If MRI was performed in the neonatal period, it would confirm that the microcephaly observed in ID and MICPCH associated with *CASK* mutations predominantly develops postnatally. Therefore, the clinical diagnosis at birth may be difficult, and assessment of postnatal growth, especially OFC, is important in the diagnostic process.

The 15 females with *CASK* mutations developed head control normally or were mildly delayed, but had marked motor delay afterwards. A large majority (13/15) could sit alone between 7 and 25 months, but only 4/15 could walk without support between 2 and 6 years. This may be related to the fact that the cerebrum in neonates was often normal in size with no cerebral malformation on MRI. As 7 of 11 patients who could not walk at their most recent

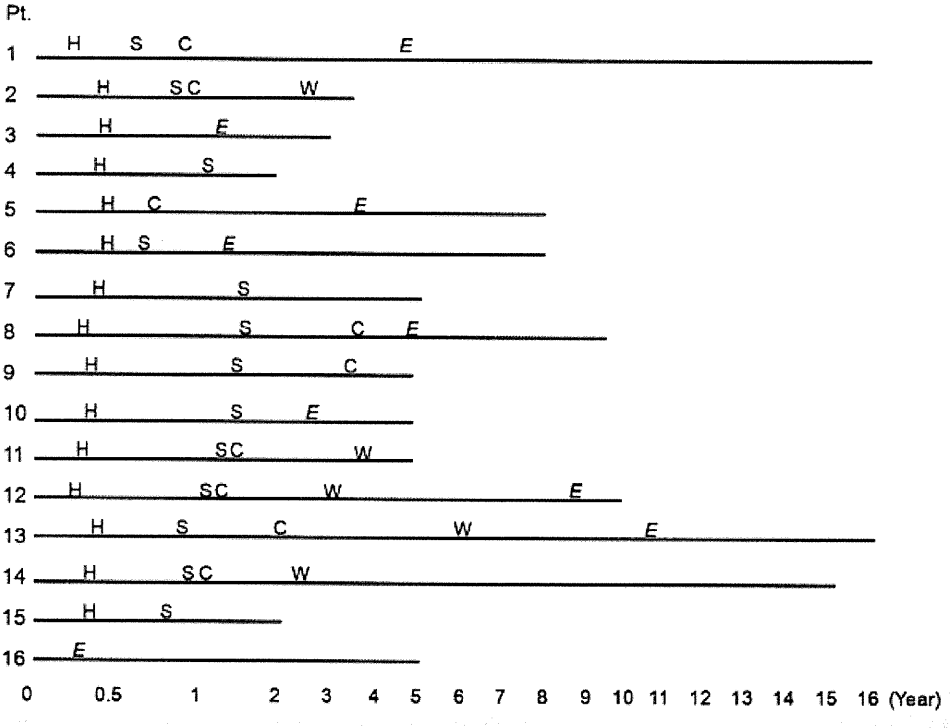

FIG. 3. Chart showing motor development and onset of epilepsy in patients with ID and MICPCH associated with *CASK* mutations. H, head control; C, crawl; S, sitting independently; W, walking independently; E, epilepsy.